ELSEVIER

Journal of Chromatography A, 853 (1999) 107–120

JOURNAL OF CHROMATOGRAPHY A

Nanoliter-scale sample preparation methods directly coupled to polymethylmethacrylate-based microchips and gel-filled capillaries for the analysis of oligonucleotides

Steven A. Soper[a,*], Sean M. Ford[a], Yichuan Xu[a], Shize Qi[a], Scott McWhorter[a], Suzzane Lassiter[a], Don Patterson[a], Richard C. Bruch[b]

[a]*Department of Chemistry, 232 Choppin Hall, Louisiana State University, Baton Rouge, LA 70803-1804, USA*
[b]*Department of Biological Sciences, Louisiana State University, Baton Rouge, LA 70803-1804, USA*

Abstract

We are currently developing miniaturized, chip-based electrophoresis devices fabricated in plastics for the high-speed separation of oligonucleotides. One of the principal advantages associated with these devices is their small sample requirements, typically in the nanoliter to sub-nanoliter range. Unfortunately, most standard sample preparation protocols, especially for oligonucleotides, are done off-chip on a microliter-scale. Our work has focused on the development of capillary nanoreactors coupled to micro-separation platforms, such as micro-electrophoresis chips, for the preparation of sequencing ladders and also polymerase chain reactions (PCRs). These nanoreactors consist of fused-silica capillary tubes (10–20 cm×20–50 μm I.D.) with fluid pumping accomplished using the electroosmotic flow generated by the tubes. These reactors were situated in fast thermal cyclers to perform cycle sequencing or PCR amplification of the DNAs. The reactors could be interfaced to either a micro-electrophoresis chips via capillary connectors micromachined in polymethylmethacrylate (PMMA) using deep X-ray etching (width 50 μm; depth 50 μm) or conventional capillary gel tubes using zero-dead volume glass unions. For our chips, they also contained an injector, separation channel (length 6 cm; width 30 μm; depth 50 μm) and a dual fiber optic, near-infrared fluorescence detector. The sequencing nanoreactor used surface immobilized templates attached to the wall via a biotin–streptavidin–biotin linkage. Sequencing tracks could be directly injected into gel-filled capillary tubes with minimal degradation in the efficiency of the separation process. The nanoreactor could also be configured to perform PCR reactions by filling the capillary tube with the PCR reagents and template. After thermal cycling, the PCR cocktail could be pooled from multiple reactors and loaded onto a slab gel or injected into a capillary tube or microchip device for fractionation.

Keywords: Microchips; DNA sequencing; Nanoreactors; Instrumentation; Sample handling; DNA; Oligonucleotides

1. Introduction

While advances in DNA separations have been numerous, for example capillary gel [1–4] and recently, microchip formats [5–10], they have out paced the development of methodologies for preparing DNA samples in a volume more commensurate with the micro-column separation techniques used to fractionate the DNAs. Standard DNA preparation protocols generate products in the μl range, therefore, not exploiting the low (nl) sample requirements for capillary and microchip separations. Low con-

*Corresponding author. Tel.: +1-504-3881-527; fax: +1-504-3883-458.
E-mail address: steve.soper@chemgate.chem.lsu.edu (S.A. Soper)

0021-9673/99/$ – see front matter
PII: S0021-9673(99)00651-2

sumable costs, for example in sequencing protocols, are of critical importance especially if it is to be financially feasible to sequence large genomes such as the human genome. For the human genome, ~75 million sequencing reactions are required (assuming a modest 400 base average read length per electrophoretic run and 10× redundancy typically required for shotgun sequencing strategies) for complete coverage. At approximately US$5.00 per reaction, the cost of reagents alone would exceed US$375·$10^6$ using conventional sample preparation methodologies.

The work presented herein describes techniques for performing several microbiological reactions on a nanoliter scale using a dynamic air thermal cycler that can accommodate capillary tubes serving as nanoreactors for applications such as PCR (polymerase chain reaction) and solid-phase DNA sequencing. The dynamic nature of the device is based upon the fact that reagents are pumped into and out of the nanoreactor using electrokinetic pumping, which is generated by the electroosmotic flow (EOF) associated with the capillary tube. The nanoreactor can be directly coupled to a capillary gel for DNA separation, providing on-line analysis of DNA fragments in an automated fashion and on a nanoliter scale. In addition, the capillary nanoreactor could be coupled to micromachined electrophoresis devices fabricated in plastics (polymethylmethacrylate, PMMA) using high-aspect ratio micromachining (HARM). Capillary connectors were directly machined into the PMMA device to allow an interface between the nanoreactor and separation device. The machining used deep X-ray etching or injection molding, which allows the fabrication of deep channels with narrow widths, appropriate for accommodating these capillary tubes [11,12].

The reactor in our examples simply consisted of a conventional fused-silica capillary tube (V~47 nl) which was placed in a thermal oven for temperature cycling. For sequencing performed in the nanoreactor, biotin was covalently attached to the wall with the subsequent addition of streptavidin to provide an anchoring point for a biotinylated DNA template prepared using PCR (solid-phase sequencing strategy). DNA sequencing using a solid support is advantageous in that it affords an easy method by which the products can be purified leading to higher efficiency separations due to the removal of excess template, primers and salts [13,14]. Solid-phase sequencing protocols have typically employed the use of magnetic beads as the support media with species attached to the support via a streptavidin–biotin linkage [15–21]. The biotin–streptavidin linkage is a suitable choice for sequencing applications due to the strength of the couple ($K_d = 10^{-15}\ M^{-1}$) which can withstand the large and rapid temperature changes necessary to perform thermal cycling.

The thermocycler constructed for this application consisted of a small chamber with heating and cooling accomplished using air. Due to the low thermal mass associated with the capillary tubes and the rapid convection associated with moving air, efficient thermal equilibration was achieved in short time periods allowing fast temperature transitions reducing the time necessary to prepare the PCR products or DNA sequencing ladders [22–24].

2. Experimental

2.1. Preparation of biotinylated DNA using PCR amplification

A 900 base pair (bp) fragment of the actin gene was obtained by PCR from rat brain RNA and cloned into a carrier vector, pCRII [3.9 kilobase pairs (kb)] (Invitrogen, San Diego, CA, USA) using previously published procedures [25]. The DNA/pCRII construct was then amplified by PCR in a Perkin-Elmer 2400 series thermocycler. The PCR mixture contained 1 μl pCRII vector, 10 μl 1X PCR buffer (20 m*M* Tris–HCl, pH 8.4, 50 m*M* KCl), 2 μl dNTPs, 85 μl double-distilled water (ddH_2O), 1 μl SP6 biotinylated forward primer (1 μ*M*) and 1 μl of T7 reverse primer (1 μ*M*). PCR was performed under ''hot start'' conditions, which entailed addition of 1 μl of the *Thermus aquaticus* (Taq) DNA polymerase (Gibco-BRL, Gaithersburg, MD, USA) after the reaction temperature reached 80°C which ensured high fidelity during DNA amplification. Twenty-five PCR cycles were performed using the following program; (1) denature dsDNA at 94°C for 45 s; (2) anneal primer at 55°C for 30 s and; (3) extend primer at 72°C for 90 s. The reaction products were separated by agarose gel electrophoresis (0.8%

agarose, 1 μ*M* EtBr, 25 V/cm) visualized under a UV lamp and excised from the gel matrix using a scalpel. The DNA was removed from the agarose using a gel removal centrifugation apparatus obtained from Amicon (Beverly, MA, USA) and stored at −20°C.

2.2. Immobilization of DNA template to reactor wall

The DNA was immobilized to the wall of a fused-silica capillary tube using a biotin–streptavidin–biotin system following procedures similar to those outlined by Amankwa and Kuhr, but with slight modifications to immobilize double-stranded (ds) DNAs instead of trypsin proteins [26,27]. Fused-silica capillary tubes (20, 50 or 100 μm I.D.×360 μm O.D.) were cut into 50 cm lengths and rinsed successively with 1 *M* NaOH, ddH_2O, 1 *M* HCl for 10 min each using a vacuum. The capillary was purged with air (10 min) and oven baked at 80°C for 10 min to remove any residual water. The capillary was then filled with a 4% solution of 3-aminopropyltriethoxysilane (APTS) in acetone, which was purchased from Sigma (St. Louis, MO, USA), for 30 min air purged for 5 min and finally incubated for 24 h at 45°C. After incubation, the tube was filled with a hydrogencarbonate solution (50 m*M*, pH 8.3) containing 5.0 mg/ml of NHS-LC-biotin (Sigma) for 4 h at room temperature. Following biotinylation, the reactor was exposed to a 4.0 mg/ml solution of streptavidin (Sigma) in 50 m*M* sodium phosphate buffer (pH 7.3). The streptavidin solution was allowed to incubate for several hours at 4°C followed by the removal of any free streptavidin by rinsing the capillary tube with ddH_2O and stored in a refrigerator until required for use. The column, when required for use, was cut to the desired length and filled with a 1 μM solution of the biotinylated template and incubated at 4°C for ~30 min. In some cases, biotinylated single-stranded (ss) DNAs were immobilized to the wall of the nanoreactor by quickly heating the dsPCR product to 95°C for several minutes followed by rapid cooling and immediately inserting the solution into the reactor. Excess template was removed by rinsing with ddH_2O and then inserted into the appropriate apparatus for evaluation and/or sequencing experiments.

2.3. DNA thermocycler

The capillary oven was designed to provide a solution to three major problems: rapid thermal cycling; good temperature accuracy and stability and; the ability to accommodate capillary tubes and dynamically move solution in and out using electrokinetic pumping. Since the working temperature range was typically between 55 and 95°C, poly(vinyl chloride) (PVC) was chosen as the oven chamber material since it provided reasonable thermal insulation, moderately low thermal capacity and was very machinable. The oven chamber measured ~15 cm in length and 1.25 cm in width. The capillary tubes were fed through the chamber via holes drilled into two ends of the oven and could accommodate 12 capillaries. Temperature-controlled air moved through the floor of the chamber through a 2.54 cm diameter hole. The chamber also contained two baffles on either side of the capillaries, which allowed the air to circulate uniformly around the capillaries. The air exited the chamber through 1/8-in. holes drilled on opposite sides of the baffles (1 in.=2.54 cm).

To heat the incoming air, a low power hot air gun heating element was used (Master Mite, 325 W). The power to the element was controlled by varying the a.c. power proportionally. To move the air through the chamber, a shaded pole, 12 CFM radial blower was used (Grainger). The ambient air was moved through the heating element mounted inside a PVC tube attached to the oven chamber entrance hole on the floor of the oven. The temperature was sensed at the oven inlet with a miniature type K thermocouple. Due to the transport lag of the system, a proportional-plus-derivative control was used to prevent temperature overshoot and ringing. The resulting system could cycle through a 40°C temperature range in ~10 s (4°C/s) to within 1°C and less than 1°C overshoot.

2.4. Nanoreactor operation

For the PCR reactions, the capillary nanoreactor (uncoated) was filled with the PCR cocktail and the

template to be amplified (λ-DNA) by inserting one end of the capillary (25 cm×20 or 50 μm I.D.) into the PCR mix and applying a high voltage (anode, positive voltage) and grounding the opposite end of the capillary. Since the thermal chamber was 15 cm in length, the volume of the PCR reaction amplified ranged from 47 to 294 nl. After filling, the applied voltage was removed and the thermal cycling commenced. Following the thermal cycling, the PCR reaction mix from all capillaries (12) was pooled to produce a reasonable volume for loading onto a gel for analysis. The PCR reactions were analyzed on an agarose gel (1%) containing ethidium bromide for visualization.

For the sequencing experiments, the biotinylated-DNA template was immobilized to the wall of the nanoreactor and the sequencing primer electroinjected into the reactor followed by rinsing and then injecting the sequencing reagents. For these experiments, the nanoreactor was ~20 cm in length (20 μm I.D.) and in order to allow electrical connection to the reactor, flanking capillaries were connected to the nanoreactor. The flanking capillaries were linear polyacrylamide (LPA)-coated using standard procedures to minimize the EOF. After primer extension, the gel-filled separation column was attached directly to the reactor using a zero dead volume connector (MicroQuartz, Phoenix, AZ, USA) with the removal of one of the flanking LPA-coated tubes. The sequencing fragments generated in the nanoreactor were then injected into the gel column for separation by applying a negative potential to the cathodic end of the LPA-coated flanking capillary.

2.5. Solid phase nano-scale sequencing reactions

The extension of the immobilized ssDNA was performed directly inside the nanoreactor. The reactor was filled with a $1 \cdot 10^{-6}$ *M* solution of IRD800-labeled T7 primer (Li-COR, Lincoln, NE, USA) and the temperature raised to 95°C followed by cooling to 55°C to allow annealing of dye-primer to the surface-immobilized template. The primer solution also contained 0.01 units of a thermophilic DNA polymerase (Taq), the four deoxynucleotides and a single dideoxynucleotide (ddCTP). In order to build a sufficient population of extension fragments to aid in detection for the capillary gel electrophoresis (CGE) experiments, the temperature of the reactor was cycled 10 times with each cycle consisting of; 92°C for 5 s; 55°C for 10 s and; 72°C for 30 s.

The matrix used for separation in the capillary was a 3% *T*/3% *C* polyacrylamide gel containing 7 *M* urea as the denaturant[1]. The field strength was set to 200 V/cm during electrophoresis and the running buffer consisted of 1× TBE (pH 8.6). The capillary gel column possessed a total length of 70 cm, with an effective length of 40 cm (injection to detection).

2.6. CGE–laser-induced fluorescence (LIF) system

The DNA fragments separated by capillary electrophoresis were detected using a custom built near-IR LIF apparatus, which was similar in design to that reported earlier by our group [28]. Basically, the system consisted of a GaAlAs diode laser producing 20 mW of laser light at 780 nm, which was focused onto the capillary using a singlet lens to a spot size of approximately 10 μm ($1/e^2$). The fluorescence was collected from the capillary with a 60× microscope objective (NA=0.85) and imaged onto a spatial filter with a slit width set to 0.6 mm which produced a sampling volume in the gel column of ~0.78 pl. After spatial filtering, the emission was spectrally filtered with an eight-cavity bandpass filter (CWL=820 nm; HBW=30 nm; Omega Optical, Brattleboro, VT, USA) and focused onto the face of the photodetector using a 20× microscope objective. The photodetector was a single photon avalanche diode (SPAD, EG&G Optoelectronics, Vadrieulle, Canada) that was passively quenched and interfaced to a personal computer which contained a counting board (CT101, Cyber Research, Bradford, CT, USA) with the data acquisition software written using LabTech Notebook[7] (Cyber Research). For the microchip fluorescence, the laser was coupled to a single mode fiber, which was then spliced into another fiber inserted and sealed into the microchip. A multimode fiber, inserted into the opposite channel of the chip, was situated directly in front of the SPAD.

[1] *C*=g *N,N′*-methylenebisacrylamide (Bis)/% *T*; *T*=(g acrylamide+ g Bis)/100 ml solution.

2.7. Fabrication of PMMA devices

PMMA micro-devices were fabricated using techniques previously outlined [11,12]. The device topography is shown in Fig. 1 (top). It basically consisted of a capillary/chip connector, a fixed volume injector (V_{inj}=100 pl), a separation channel (L=6 cm) and two channels to accommodate optical fibers for delivering the laser light to the device and also collecting the emission and directing it to the photon transducer. In Fig. 1 (bottom) is shown a scanning electron microscopy (SEM) image of the dual fiber detector fabricated in PMMA.

3. Results and discussion

3.1. PCR amplification in nanoreactor

Our initial investigations focused on evaluating the performance of the nano-PCR reactor. For these investigations, we used 50 μm I.D. capillaries filled with the PCR cocktail and template. Following amplification, the PCR mixes from the 12 capillaries were pooled. Fig. 2 shows the electropherogram of the amplicons obtained from the nano-thermal cycler and a conventional thermal cycler. The PCR product generated in the nanoreactor co-migrated with the conventional PCR product, both matching the appropriate DNA size marker (603 bp fragment of *Hae III* digest of ΦX174), confirming the molecular mass of the amplicon. Monitoring the nano-oven temperature profile during thermal cycling indicated little evidence of overshoot, except at 72°C, where the temperature overshot by ~2°C, but still within a reasonable temperature range to get efficient extension. In addition, the temperature was found to be very stable (±1.0°C).

3.2. DNA sequencing in nanoreactor

The efficiency of DNA immobilization onto the capillary wall was initially studied using a large diameter nanoreactor (5 cm length×100 μm I.D.) which generated sufficient product volumes allowing off-line analysis using scintillation counting. The degree of surface coverage was determined by incorporating a ^{32}P label into the template, which contained the biotin linkage at the 5′ terminus and was bound to the wall-immobilized streptavidin species. The amount of activity generated from the reactor was then measured by submerging the entire reactor into a vial containing a scintillation cocktail and monitoring the activity using the scintillation counter. The theoretical scintillation intensity for complete monolayer coverage was determined by calculating the surface area available for immobilization inside the reactor and assuming that the degree of coverage was restricted by the area occupied by the streptavidin protein (2000 Å^2) [26,27]. The coupling ratio of biotinylated DNA to the streptavidin anchor was assumed to be 1:1 due to steric interactions that would result when multiple 1 kbp templates would bind to a single immobilization site. Based on these assumptions, the efficiency of template immobilization to the interior reactor wall was determined to be 77% (±10%). From the physical dimensions of this reactor (5 cm length×100 μm) the average amount of DNA immobilized in this system was ~$1\cdot10^{-12}$ mol yielding an effective DNA concentration of $2.6\cdot10^{-6}$ M in this 390 nl volume.

Integration of the nanoreactor directly to a capillary gel column for sequencing requires careful consideration to zone broadening due to extra-column effects because of the stringent requirements on separation efficiency in sequencing applications in order to achieve single-base resolution. In the present case, the finite volume of the reactor (injection volume, V_{inj}, for a 15 cm×20 μm I.D. column, V_{inj}=47 nl) and the dead volume associated with the connector can potentially result in the reduction in the plate numbers. In order to assess the contributions of these two variances to the total variance, experiments were carried out to evaluate the relative contribution from the connector (σ^2_{con}) and reactor volume (σ^2_{inj}). This extra column variance (σ^2_{xc}) can be calculated from the following expression, assuming that the zone variance from the finite injection volume could be calculated from $l^2/12$ [29], where l is the length of the injection plug;

$$\sigma^2_{xc} = \left[\frac{\mu^2_{gel}}{12\mu^2_{fs}} \cdot \frac{r^4_{nr}}{r^4_{sc}} \cdot l^2_{nr} \right] + \sigma^2_{con} \quad (1)$$

where μ_{gel} is the electrophoretic mobility of the oligonucleotide in the gel column; μ_{fs} is the free

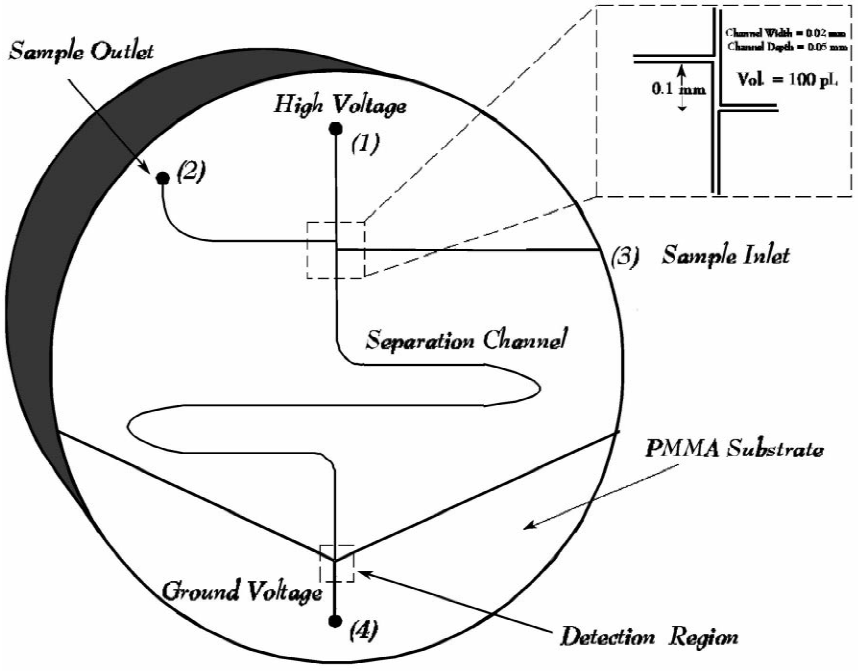

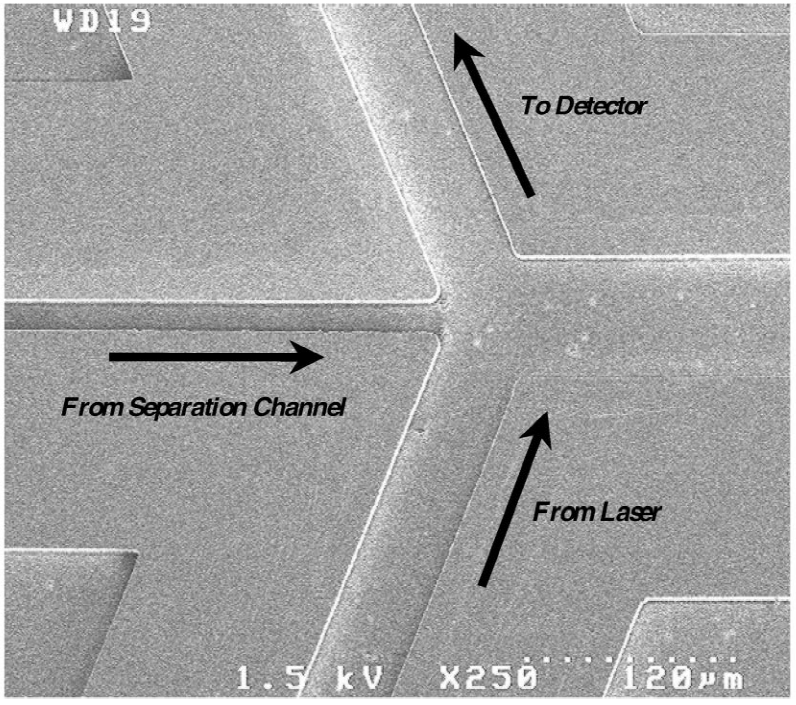

Fig. 1. Topographical layout of the micro-electrophoresis chip fabricated in PMMA (top). The channels were 50 μm in depth and varied in width (20 μm or 50 μm). The injector contained a volume of 100 pl. (Bottom) SEM image of dual fiber-optic component micromachined in PMMA.

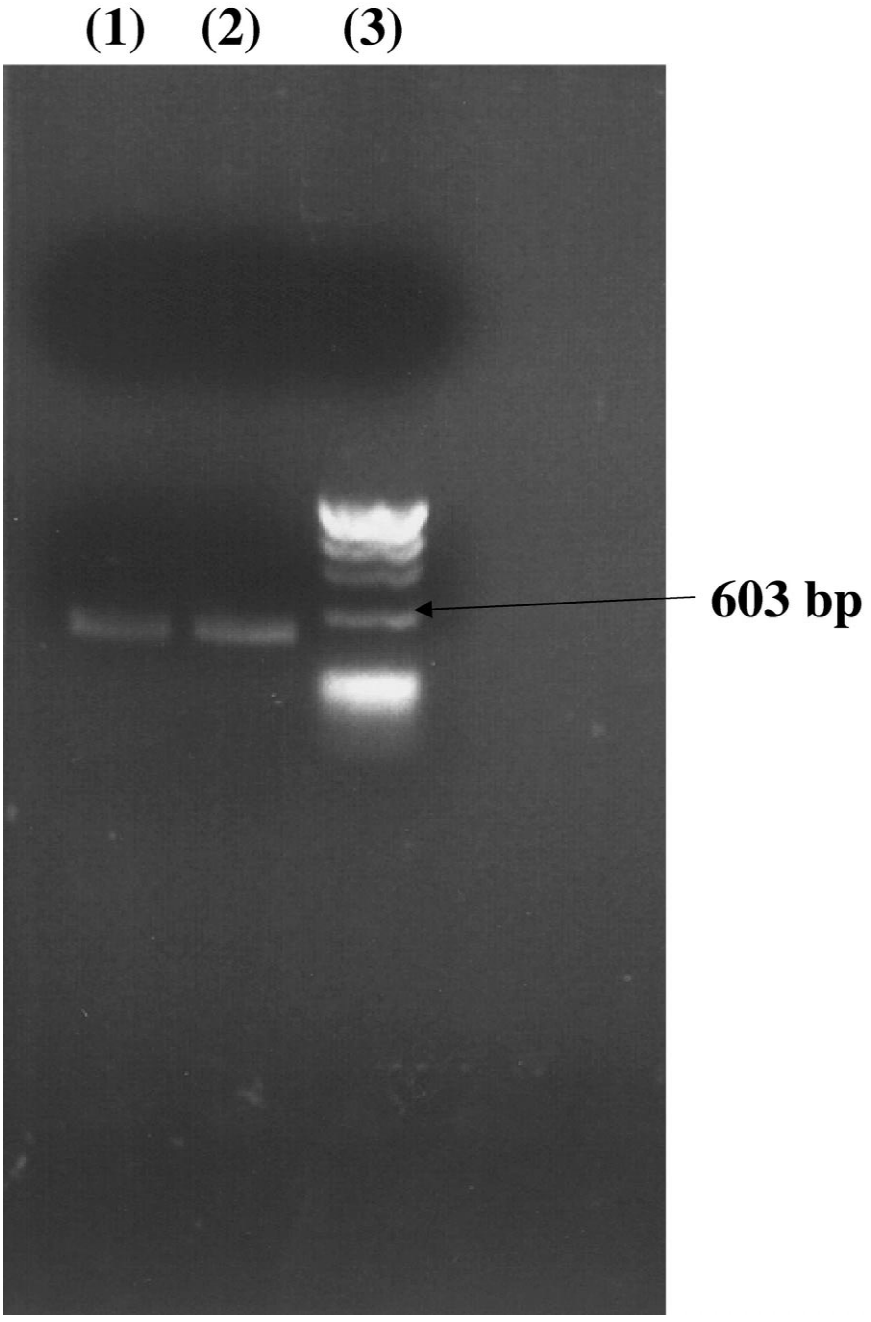

Fig. 2. Image of agarose gel (1%) electropherogram of λ-DNA amplified in both a conventional thermal cycler (PE 2400, Applied Biosystems) (lane 1) and the dynamic nano-thermal cycler (lane 2). The PCR mix contained AmpliTaq DNA polymerase, Tris–HCl (100 m*M*, pH 8.3), KCl (500 m*M*), $MgCl_2$ (15 m*M*) and the following primers: (1) 5′-GATGAGTTCGTGTCCGTACAACTGG-3′; (2) 5′-GGTTATCGAAATCAGCCACAGCGCC-3′. These primers produced a 500 bp amplicon. The thermal cycle consisted of 95°C 15 s; 55°C 15 s; 72°C 60 s; 30 cycles followed by a final extension for 5 min at 72°C. Lane (3) contains a marker ladder (*Hae III* digest of ΦX174).

solution mobility of the oligonucleotide ($4.0 \cdot 10^{-4}$ $cm^2/V\ s$) [30]; r_{nr} is the radius of the nanoreactor; r_{sc} is the radius of the separation capillary and l_{nr} is the length of the nanoreactor. The term in parentheses represents the zone variance arising from the finite injection volume (σ^2_{inj}) and assumes that complete radial diffusion occurs when injecting into a column with a larger radius. As can be seen from this expression, in order to minimize σ^2_{inj}, it is necessary to use a highly crosslinked gel or high % *T* linear gel (small μ_{gel}) and also a small diameter nanoreactor and larger diameter separation column. It should also be noticed from Eq. (1) that the zone variance from σ^2_{inj} will be highly dependent upon the number of bases comprising the oligonucleotide, since the longer oligonucleotides have a smaller μ_{gel}. In the present case, $\mu_{gel} < \mu_{fs}$ and $r_{nr} < r_{sc}$, and therefore, zone compression should result when injecting the contents of the nanoreactor directly into the gel column.

The zone variance from the connector was determined by loading the nanoreactor with dye-labeled primer and interfacing it via the glass connector to a gel-filled column followed by electrokinetically injecting the dye-primer onto the gel column. The electropherogram generated using this arrangement was compared to one generated after performing a direct injection of near-IR dye-primer onto the CGE column under similar electrokinetic injection conditions. In both cases, the injection volume was kept constant, which was accomplished, in the case of the connector experiment, by removing the separation capillary and placing it in 1X TBE once the appropriate injection volume had been reached. The plate numbers (data not shown) were found to be $2.49 \cdot 10^5$ plates for direct injection and $2.45 \cdot 10^5$ plates when injection occurred across the zero dead volume connector. Since the only additional contribution to the zone variance was that arising from the connector between these two cases, the difference in the total zone variance calculated from the electropherograms yielded σ^2_{con}, which was determined to be $1.5 \cdot 10^{-4}$ cm^2. Even though the connector is stated as possessing zero dead volume, the loss in efficiency in this case is most likely due to the inability to polish the capillary ends correctly, producing a void volume at the interface.

The nanoreactor used in our sequencing experiments was selected to have a length of 15 cm (l_{nr}) and radius of 10 μm (r_{nr}), yielding a total volume of 47 nl. From previous measurements, we found that the mobility of a 150mer in a 3% *T*/3% *C* polyacrylamide gel with a near-IR primer was $6.1 \cdot 10^{-5} cm^2/V\ s$ [31]. Using these numbers as well as the free solution mobility of an oligonucleotide with >20 bases yielded a value of $3.4 \cdot 10^{-3}$ cm^2 for σ^2_{nr}. The total variance (σ^2_{tot}) for this 150mer near-IR labeled single stranded oligonucleotide using direct injection onto a cross-linked gel column was found to be $1.3 \cdot 10^{-3}$ cm^2 ($H_{tot} = 2.5 \cdot 10^{-5}$ cm, where *H* is the height equivalent of a theoretical plate) and the plate number was $2.0 \cdot 10^6$ [31]. Adding the zone variance contributions from the connector and the injection volume produced by the nanoreactor would give an estimate on the efficiency of this injection system, which yielded a value of $4.8 \cdot 10^{-3}$ cm^2 ($H_{tot} = 8.6 \cdot 10^{-5}$ cm) and a plate number of $5.8 \cdot 10^5$. Therefore, one could expect an approximate 65% reduction in separation efficiency using the injection system as configured above compared to direct injection.

Fig. 3 shows the capillary electropherogram for C-terminated fragments generated in the nanoreactor with subsequent separation in a 3% *T*/3% *C* cross-linked polyacrylamide gel column (75 μm I.D.). From this electropherogram, we estimated an effective read length of approximately 450 bases, which was determined by peak counting and then multiplying by 4 to a point in the electropherogram where resolution permitted single base identification ($R > 0.7$). However, it should be noted that since only the C-track was analyzed, the stated read length will most likely be reduced when the system is transferred to a single lane, four base protocol. Calculation of the plate number for the near-IR dye-labeled 160mer depicted in the figure inset yielded a value of $2.05 \cdot 10^6$ plates compared to $4.51 \cdot 10^6$ plates for direct injection (data not shown), in fair agreement to the efficiency loss calculated above. An interesting feature of this injection format is the fact that biases due to electrokinetic injection are absent, since in the present case we are injecting onto the gel column a fixed volume, which is defined by the physical dimensions of the capillary nanoreactor.

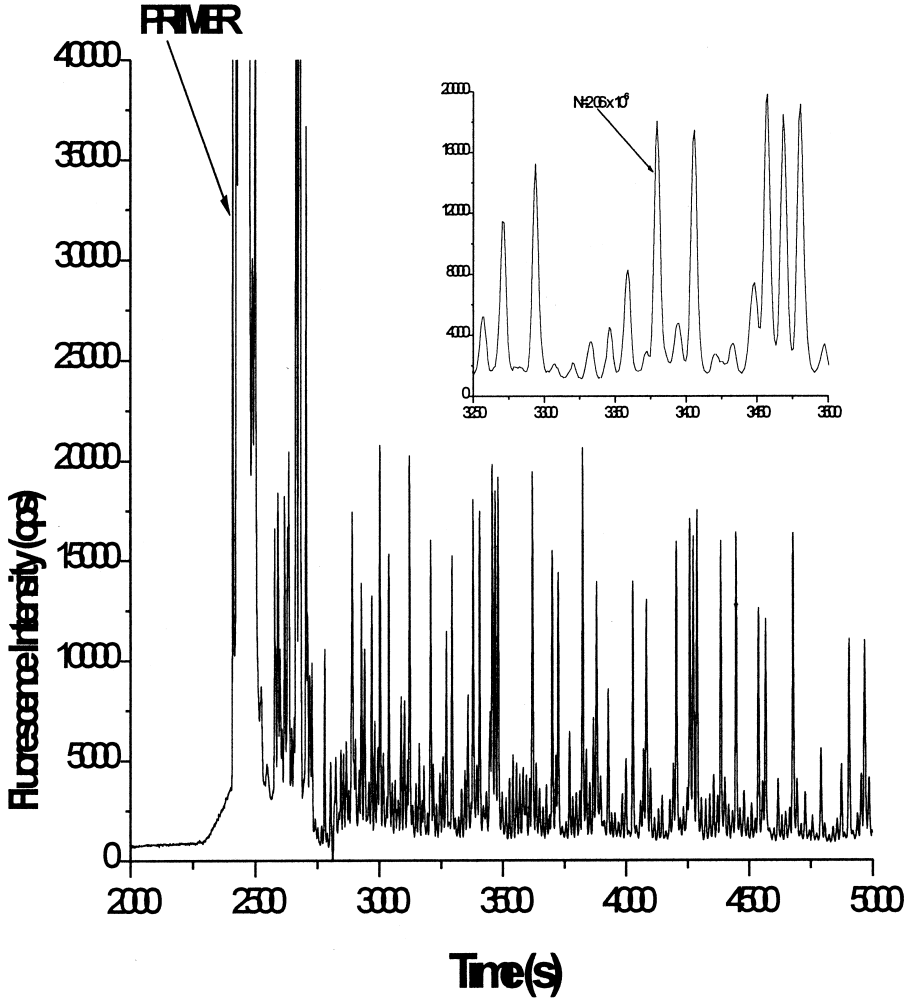

Fig. 3. Capillary gel electropherogram of C-terminated Sanger sequencing fragments produced in the nanoreactor possessing an approximate volume of 47 nl. The fluorescence of the labeling dye was excited with 4.5 mW of laser power at 780 nm. The column length, injector to detector, was 40 cm with a total length of 70 cm. The electrophoresis was carried out using a field strength of 200 V/cm. The graph inset shows an expanded view with the 160mer labeled with the plate numbers calculated for this peak. In the figure, only 5000 s of data are shown.

3.3. Microchip separations and interconnection to capillaries

In order to investigate the ability to carry out high resolution separations of oligonucleotides using our PMMA-based micro-device with no wall coatings, we electrophoresed a near-IR labeled primer using a 4% LPA sieving matrix in both a PMMA-based micro-device and a conventional fused-silica capillary which was modified with a 1% LPA coated wall. The results are shown in Fig. 4. As can be seen, the primer migrated through the fused-silica capillary column in approximately 1720 s, while for the PMMA-based device, the migration time was only 194 s, an approximate 10-fold decrease in migration time. For the fused-silica case, the apparent mobility of the dye-labeled primer in this gel matrix was found to be $8.46 \cdot 10^{-5}$ $cm^2/V\,s$, while in the case of

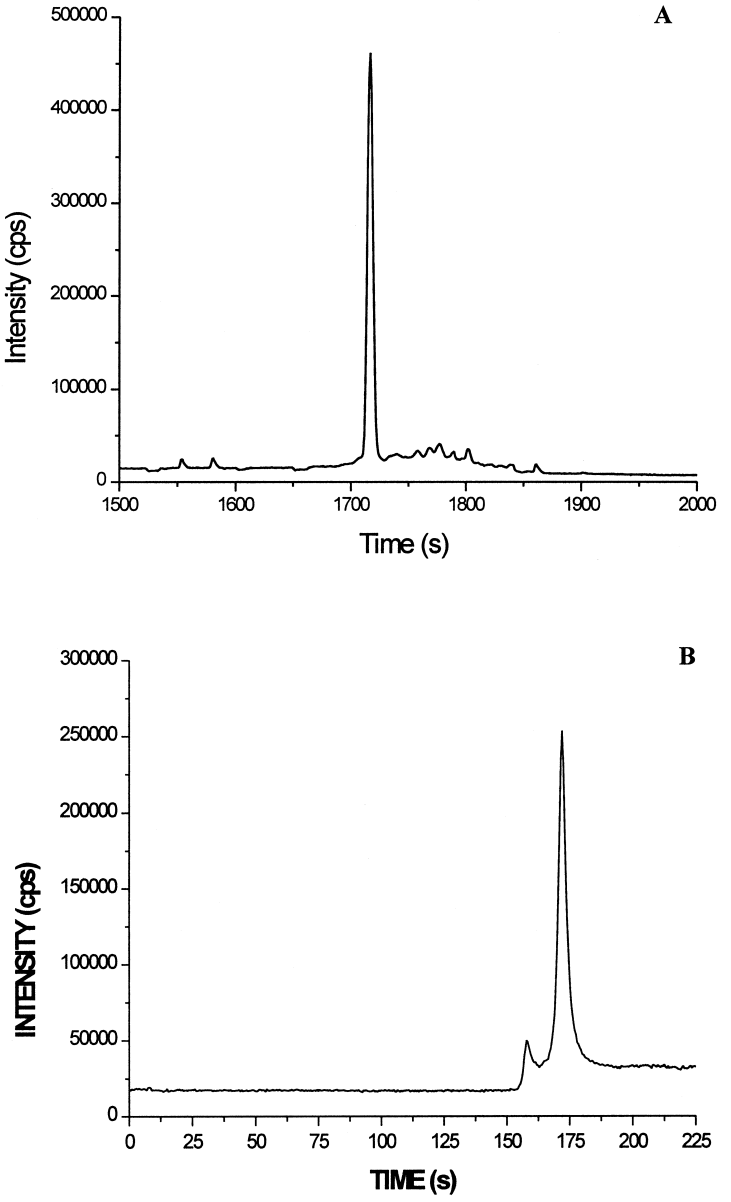

Fig. 4. Electrophoretic separations of near-IR dye-labeled sequencing primers in a conventional capillary tube (A) or PMMA-based microchip (B). The labeling dye was NN382 (Li-COR, Lincoln, NE, USA) and the primer was an M13 (-21) primer. The sieving matrix was a 4% LPA solution containing 7 *M* urea as the denaturant. For the capillary gel separation, the wall was coated with a 1% LPA solution while for the microchip separation, the device walls were not modified.

the PMMA-based device, the apparent mobility was determined to be $7.44 \cdot 10^{-5}$ cm^2/V s. The lower mobility observed in the case of the PMMA-based device most likely resulted from the fact that the EOF, which opposes the electrophoretic mobility of the dye-labeled oligonucleotide, in the PMMA device is larger than for the wall-coated fused-silica tube. We also calculated the plate numbers generated from these two separations and found that the plate numbers in the fused-silica case was 836 000 plates/

m, while for the PMMA device, the plate numbers were 722 000 plates/m. The slight loss in efficiency may arise from either the turns used to increase the channel length or the finite length of the injection plug or a combination of both. Recently, a model has been formulated to account for dispersion effects introduced by turns in the separation channel of microchips [32]. The important conclusion from this model was that narrow channels were critical so as to reduce path differences taken by individual molecules.

In order to estimate the zone variance introduced by the turns (σ_t^2) in our device, we calculated the diffusion coefficient (D) of the dye-labeled primer from the capillary gel electropherogram, since the major contribution to the total variance is longitudinal diffusion (σ_D^2) in this case. Since the diffusion coefficient has been shown to depend on the applied electric field [33], the same field strength was used in the microchip as that in the capillary gel electrophoresis case. After obtaining D and using the physical dimensions of our micro-device, we could calculate σ_t^2. From the electropherogram depicted in Fig. 4A, the total variance was determined to be $4.79 \cdot 10^{-3}$ cm^2, which yielded a value of $1.39 \cdot 10^{-6}$ cm^2/s for the diffusion coefficient. The total zone variance for the electrophoretic peak shown in Fig. 4B was determined to be $5.54 \cdot 10^{-4}$ cm^2. Insertion of the value calculated for the diffusion coefficient into the expression,

$$\sigma_D^2 = \frac{2DL}{\nu_{ave}} \quad (2)$$

where L is the effective length of the separation channel and ν_{ave} is the average linear velocity, allowed the determination of σ_D^2 which was found to be $5.14 \cdot 10^{-4}$ cm^2, comprising approximately 93% of the total variance. Insertion of the appropriate values into Eq. (14) found in Ref. [32], yielded a value of $8.66 \cdot 10^{-6}$ cm^2 for σ_t^2, or a total turn variance per device (three turns) of $2.60 \cdot 10^{-6}$ cm^2. From the 100 μm injection plug length used for sample injection, we could also calculate σ_{inj}^2, which was determined to be $8.31 \cdot 10^{-6}$ cm^2. As can be seen, the injection plug variance is nearly four-fold greater than the variance per turn. It should be noted that microscopic visualization of the injection process for our device indicated significant leakage of sample into the separation channel during injection. Therefore, the 100 μm plug length used in these calculations should be considered provisional. Use of a pinched injection mode should alleviate this artifact and improve the plate numbers [34]. These calculations demonstrate the need for the fabrication of channels with narrow widths and deep depths to minimize zone variances caused by turns and also to produce a channel with a reasonable volume to allow sample loading levels to aid in detection.

The limit of detection of our fluorescence system was estimated by calculating the S/N of the electrophoretic peak shown in Fig. 4B, which was determined by calculating the area under this peak and dividing by the square root of the number of background counts integrated over the time width of this peak. Calculation of the S/N was found to be 250 for an injection of 100 pl of a 1.0 nM solution of the dye-primer, which represents 0.1 amol. At a $S/N = 3$, our detector possesses a mass detection limit of 1.2 zmol, which compares favorably to our detection limits determined for a capillary-based system using near-IR fluorescence [28].

For connecting the capillary nanoreactor to the microchip, we have machined guide channels to hold the capillary tubes. Since the capillary wall is several microns thick and we needed to reduce unswept volumes (void volumes) at the interface of the chip to the capillary, the guide channel was 50 μm in width and abruptly reduced to 20 μm in width since the capillary inserted into the device had an internal diameter of 20 μm. Fig. 5 shows an optical micrograph of a 20 μm I.D. capillary inserted into the PMMA-based device. The capillary possessed an O.D. of ~55 μm and therefore, did not require etching to reduce its outer diameter so as to fit into this narrow channel. The capillary was positioned into the guide channel using a micro-translational stage while observing the movement under an optical microscope. After insertion, the capillary was simply glued (using epoxy) to the PMMA-micro-device.

4. Conclusions

We have demonstrated the ability to effectively produce PCR reactions and sequencing ladders on a

Fig. 5. Optical micrograph of a fused-silica capillary inserted into a micro-channel fabricated in PMMA. The capillary possessed an O.D. of 55 μm and an I.D. of 20 μm.

nanoliter-scale, a volume which exploits the small sample requirements associated with micro-column separation techniques. The system uses nano-fluidics for dynamically moving reagents and sample into the reactor (electrokinetic pumping). The volume used in the present system for preparing sequencing ladders (~47 nl) represents an approximate 300-fold reduction in sample size typically used in Sanger chain-termination protocols. The net result is a significant reduction in the amount of consumables required for generation of sequencing ladders. A cost analysis for large-scale DNA sequencing applications using standard protocols and the DNA nanoreactor system indicated that reagent costs could run as high as US$12 750 per day when performing 2500 sequencing reactions (for an average read length of 400 bases per electrophoretic run, this corresponds to $1 \cdot 10^6$ bases of raw sequencing data per day) compared to only US$40.65 per day when using the nanoreactor. Another attractive feature of this system is the ability to perform solid-phase sequencing in ultra-small volumes with its incumbent advantages,

such as removal of excess primer, salts and dNTPs prior to separation, improving banding in the electropherogram. In addition, since the anchor used in the present system is stable toward typical sequencing conditions, one can subject the immobilized DNA template to multiple sequencing rounds making it amenable to such techniques as primer walking. Our preliminary data has indicated that we can subject the immobilized template to four to five rounds of sequencing before seeing a significant reduction in signal. However, for a four-base, single lane format, this methodology will require the use of dye-labeled terminators (dideoxynucleotides) and not dye-labeled primers as used here. The use of dye-labeled primers would require four nanoreactors with subsequent pooling of the reaction products prior to separation. Work in our laboratory is currently focused on developing near-IR dye-labeled terminators for use in the nanoreactor system.

We have also demonstrated the ability to fabricate micro-electrophoresis devices in PMMA using high-aspect ratio micromachining, with these devices containing such components as fixed volume injectors, integrated fiber optic fluorescence detectors and guide channels to interconnect capillary tubes to the microchip for simplifying loading and interfacing to capillary nanoreactors. Our data has demonstrated that these devices can fractionate oligonucleotides in LPA matrices with reduced times compared to conventional capillary electrophoresis and still generate similar plate numbers. In addition, due to the low electroosmotic flow that these devices generate, the wall of the device need not be polymer-coated, potentially extending the operational lifetime of the device. Integration of our capillary-based nanoreactor systems with these PMMA microchips will allow the fabrication of automated devices for analyzing DNA which consume minute amounts of costly reagents.

Acknowledgements

Financial support of this work by the NIH (HG01499) is greatly appreciated. The authors would also like to thank Dr. Huigen Dong for helpful discussions during the course of this work.

References

[1] H. Drossman, J.A. Luckey, A. Kostichka, J. D'Cuhna, L.M. Smith, Anal. Chem. 62 (1990) 900–903.
[2] N.J. Dovichi, in: J.P. Landers (Ed.), Handbook of Capillary Electrophoresis, CRC Press, Boca Raton, FL, 1994, pp. 369–387.
[3] A.S. Cohen, D.L. Smisek, P. Keohavong, Trends Anal. Chem. 12 (1993) 195–202.
[4] C.A. Monnig, R.T. Kennedy, Anal. Chem. 66 (1994) 280R–314R.
[5] C.S. Effenhauser, A. Manz, H.M. Widmer, Anal. Chem. 65 (1993) 2637–2642.
[6] A.T. Woolley, R.A. Mathies, Anal. Chem. 67 (1995) 3676–3680.
[7] S.C. Jacobson, J.M. Ramsey, Anal. Chem. 68 (1996) 720–723.
[8] A.T. Woolley, R.A. Mathies, Proc. Natl. Acad. Sci. 91 (1994) 11348–11352.
[9] A.T. Woolley, D. Hadley, P. Landre, A.J. DeMello, R.A. Mathies, M.A. Northrup, Anal. Chem. 68 (1996) 4081–4086.
[10] D. Schmalzing, L. Koutny, A. Adourian, P. Belgrader, P. Matsudaira, D. Ehrlich, Proc. Natl. Acad. Sci. 94 (1997) 10273–10278.
[11] S.M. Ford, B. Kar, S. McWhorter, J. Davies, S.A. Soper, M. Klopf, G. Calderon, V. Saile, J. Microcol. Sep. 10 (1998) 413–422.
[12] S.M. Ford, J. Davies, B. Kar, S.D. Qi, S. McWhorter, S.A. Soper, J. Biomech. Eng. 121 (1999) 1–8.
[13] X. Tong, L.M. Smith, Anal. Chem. 64 (1992) 2672–2677.
[14] X. Tong, L.M. Smith, Seq. Map. 4 (1993) 151–162.
[15] T. Hultman, S. Stahl, T. Moks, M. Uhlen, Nucleos. Nucleot. 7 (1988) 629–638.
[16] R. Ohara, O. Ohara, DNA Res. 2 (1995) 123–129.
[17] S. Stahl, T. Hultman, A. Olsson, T. Moks, M. Uhlen, Nucl. Acids Res. 16 (1988) 3025–3038.
[18] T. Hultman, S. Stahl, E. Hornes, M. Uhlen, Nucl. Acids Res. 17 (1989) 4937–4946.
[19] M. Uhlen, Nature 340 (1989) 733–734.
[20] T. Hultman, S. Bergh, T. Moks, M. Uhlen, BioTechniques 10 (1991) 84–93.
[21] S.-C. Haung, H. Swerdlow, K.D. Caldwell, Anal. Biochem. 222 (1994) 441–449.
[22] C.T. Wittwer, D.J. Garling, D.R. Hillyard, Nucl. Acids Res. 17 (1989) 4353–4357.
[23] C.T. Wittwer, G.C. Fillmore, D.J. Garling, Anal. Biochem. 186 (1990) 328–331.
[24] H. Swerdlow, K. Dew-Jager, R.F. Gesteland, BioTechniques 15 (1993) 512–519.
[25] R. Bruch, K. Medler, NeuroReport 7 (1997) 2941–2944.
[26] L.N. Amankwa, W.G. Kuhr, Anal. Chem. 64 (1992) 1610–1613.
[27] L.N. Amankwa, W.G. Kuhr, Anal. Chem. 65 (1993) 2693–2697.

[28] B.L. Legendre, D.L. Moberg, D.C. Williams, S.A. Soper, J. Chromatogr. A 779 (1997) 185–194.
[29] J.C. Sternberg, Adv. Chromatgr. 2 (1966) 205–211.
[30] P.D. Grossman, J. Colburn, Capillary Electrophoresis – Theory and Practice, Academic Press, New York, 1992.
[31] D.C. Williams, S.A. Soper, Anal. Chem. 67 (1995) 4358–4365.
[32] C.T. Culbertson, S.C. Jacobson, J.M. Ramsey, Anal. Chem. 70 (1998) 3781–3789.
[33] D. Schmalzing, A. Adourian, L. Koutny, L. Ziaugra, P. Matsudaira, D. Ehrlich, Anal. Chem. 70 (1998) 2303–2310.
[34] S.C. Jacobson, R. Hergenröder, L.B. Koutny, J.M. Ramsey, Anal. Chem. 66 (1994) 1114–1118.